Macromolecules

COMMUNICATION TO THE EDITOR

pubs.acs.org/Macromolecules

Three-Dimensional Assembly of Gold Nanoparticles in Spherically Confined Microphase-Separation Structures of Block copolymers

Hiroshi Yabu,[†,‡,*] Tatsuya Jinno,[§] Kazutaka Koike,[§] Takeshi Higuchi,[⊥] and Masatsugu Shimomura[†,⊥]

[†]Institute of Multidisciplinary Research for Advanced Materials (IMRAM), Tohoku University, 2-1-1, Katahira, Aoba-Ku, Sendai 980-8577, Japan

[‡]Precursory Research for Embryonic Science and Technology (PRESTO), Japan Science and Technology Agency (JST), 4-1-8, Honcho, Kawaguchi, Saitama 332-0012, Japan

[§]Graduate School of Engineering, Tohoku University, 2-1-1, Katahira, Aoba-Ku, Sendai 980-8577, Japan

[⊥]WPI-Advanced Institute for Materials Research (AIMR), Tohoku University, 2-1-1, Katahira, Aoba-Ku, Sendai 980-8577, Japan

Supporting Information

ABSTRACT: Three-dimensional (3D) assemblies of metal nanoparticles are promising materials for plasmonic materials. Metal nanoparticles have unique surface plasmon resonances, ranging from ultraviolet to visible light wavelengths, depending on their metal species, size, and shape. The arrangements and spacing of the nanoparticles also strongly affect the plasmonic properties. The microphase separation of block copolymers can create a nanoscopic periodic structure, where metal nanoparticle assemblies are arranged along the microphase separation structure. In this paper, we construct 3D Au nanoparticle assemblies embedded in the microphase separation structures of confined block copolymers, in the pores of inverse opals. Polymer-stabilized Au nanoparticles were synthesized, and submicrometer poly(styrene) (PS) colloidal crystals were prepared using a simple coating method. After molding a PS colloidal crystal with poly(vinyl alcohol) (PVA), block copolymers and Au nanoparticles were introduced into the PVA inverse opal from solution. The inner nanostructures were analyzed by transmission electron microscopy (TEM).

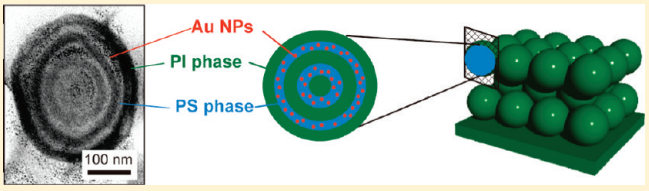

1. INTRODUCTION

Three-dimensional (3D) assemblies of metal nanoparticles are promising materials for plasmonic materials, such as highly sensitive surface enhanced Raman scattering (SERS) substrates,[1] plasmonic crystals,[2] and metamaterials for visible light optics,[3] among others.[4] Metal nanoparticles have unique surface plasmon resonances, ranging from ultraviolet to visible light wavelengths, depending on their metal species, size and shape.[5] The arrangements and spacing of the nanoparticles also strongly affect the plasmonic properties.[6] Many methods for arranging metal nanoparticles onto two-dimensional (2D) solid substrates have been developed that employ top-down microfabrication techniques including electron beam lithography,[7] photolithography,[8] nanoimprint lithography,[9] and so on.[10] However, it is difficult and time-consuming to create 3D arrays of metal nanoparticles by using conventional lithographic technologies.

Bottom-up approaches for arranging metal nanoparticles into 2D periodic arrays also have been reported. The Langmuir−Blodgett technique can be used for preparing 2D crystals of fine metal nanoparticles.[11] Spatz et al. reported that 2D arrays of block copolymer micelles, which contained metal nanoparticles, were fabricated on a Si substrate using a simple dip-coating method.[12] For creating 2D arrays of metal nanoparticles other methods employing dewetting,[13] supramolecular interactions,[14] and DNA-mediated assemblies[15] have also been reported. However, the 3D arrangement of metal nanoparticles is still a challenge. Three-dimensional assemblies of metal nanoparticles are required in order to construct ideal plasmonic materials with broad-band absorption, high resonance efficiency, and no angular dependence.

Block copolymer microphase separation structures are good candidates for the bottom-up approach to arranging metal nanoparticles. Recent developments in living polymerization have allowed the preparation of a wide variety of block copolymers which have a high affinity for metal nanoparticles and form unique microphase separation structures. Many studies have been published detailing the assembly of metal nanoparticles in 2D and 3D microphase separation structures in bulk or thin film block copolymers.[16] The microphase separation of block copolymers can create a nanoscopic periodic structure, where metal nanoparticle assemblies are arranged along the microphase separation structure. However, the orientation of the microphase separation structure's nanodomain which contains the metal nanoparticles cannot be controlled, and the domain sizes of the microphase separation structures are too small for optical and electrical applications. Mesoscopic templates avoid these problems by arranging the nanodomains of the microphase separation structures.[17] The microphase separation structures were arranged along

Received: May 2, 2011
Revised: June 14, 2011
Published: July 05, 2011

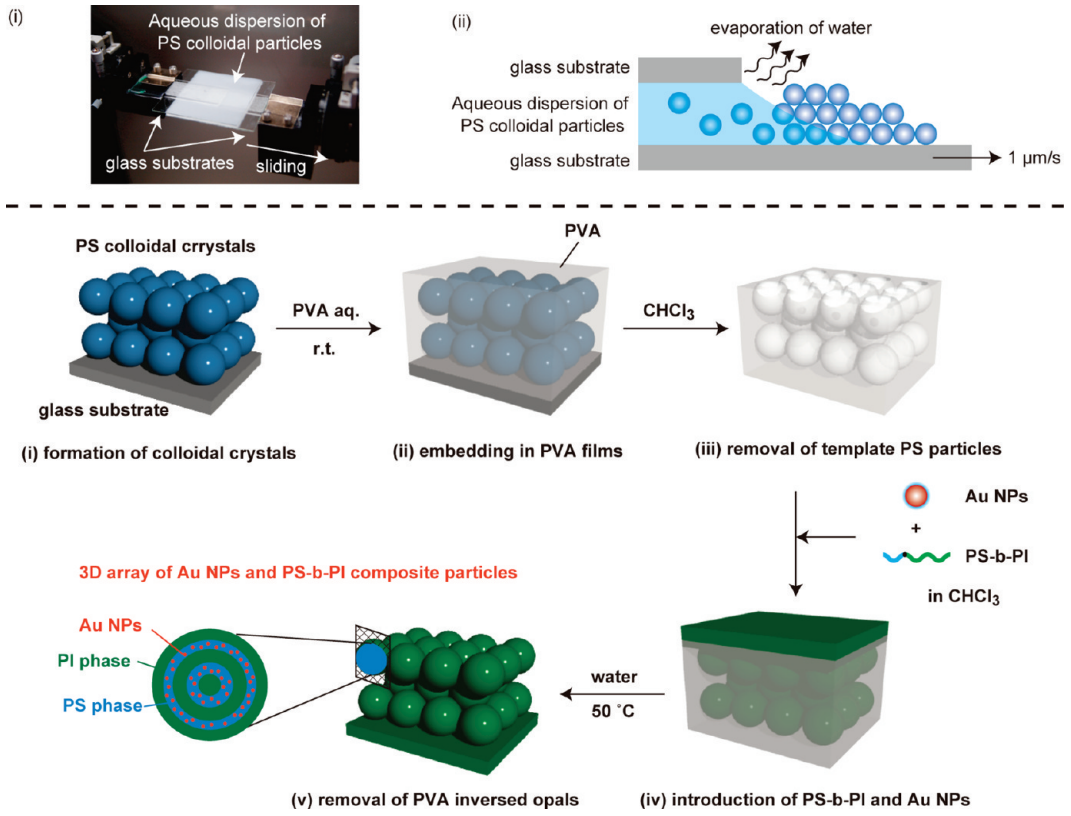

Figure 1. (a) Photograph of coating apparatus (i) and the schematic illustration of colloidal crystal preparation (ii). (b) Schematic illustration of preparation method of inverse opals and Au nanoparticles and block copolymer composites.

the interface between the template and the block copolymer; the structure depended on the boundary conditions and size of the confined space in the template.[18] Thin film (1D) confinement,[19] 2D confinement systems,[20] and 3D confinement have previously been reported.[21]

Inverse opals are suitable templates for 3D confinement systems because their pore size is comparable to the characteristic length of the microphase separation in block copolymers. Dispersions of submicrometer- or micrometer-sized colloidal particles can be assembled into fine crystals by evaporation of solvent,[22] spin-coating[23] or compression.[24] After molding the colloidal crystals with another material and removing the template colloid, inverse opals can be prepared.[25] By using colloidal crystals and inverse opals as confinement spaces, frustrated block copolymer microphases can be created.[26]

In this paper, we construct 3D Au nanoparticle assemblies embedded in the microphase separation structures of confined block copolymers, in the pores of inverse opals. Polymer-stabilized Au nanoparticles were synthesized according to a variation of the method reported by Brust et al.[27] Submicrometer poly(styrene) (PS) colloidal crystals were prepared using a simple coating method. After molding a PS colloidal crystal with poly(vinyl alcohol) (PVA), block copolymers and Au nanoparticles were introduced into the PVA inverse opal from solution. The inner nanostructures were analyzed by transmission electron microscopy (TEM).

2. EXPERIMENTAL SECTION

2.1. Synthesis of Au Nanoparticles. A toluene solution (synthetic grade, 30 mL, 5 mM) of tetraoctyl ammonium bromide ($C_8H_{17}NBr$, Aldrich, USA) was added to a 2.5 mM solution of hydrogen tetrachloroaurate(III) tetrahydrate ($HAuCl_4 \cdot 4H_2O$, Wako/GR, Japan) in deionized water (20 mL). Soon after the addition, the yellow aqueous phase became colorless, and the organic phase turned orange. This color change implies that the gold ions were transferred from the aqueous phase to the organic phase. A 2.5 mM solution of thiol-terminated poly(styrene) (PS-SH, M_n = 3.0 kg/mol, M_w/M_n = 1.07, Polymer Source Inc., Canada) was prepared and added to the solution. An aqueous solution (10 mL, 0.5 M) of sodium tetraborohydride ($NaBH_4$, Wako/GR, Japan) was slowly added to the water/toluene solution with vigorous stirring. After the $NaBH_4$ solution was thoroughly mixed, the solution was stirred for 2 h. The toluene phase turned deep red, which indicates the formation of Au nanoparticles, shortly after the addition of the $NaBH_4$ solution. The toluene phase was extracted by decantation, and the Au nanoparticles were precipitated by the addition of ethanol (50 mL, Wako/GR, Japan) at 2 °C. The Au nanoparticles were collected by centrifugation, and then used to prepare a 20 mg/mL dispersion in chloroform.

The absorption spectrum of the Au nanoparticle dispersion was acquired by UV−vis spectroscopy (V-670, Jasco), and the Au nanoparticles were observed by TEM (H-7650, Hitachi, Japan). The solution of Au nanoparticles (1 μL) was cast on a Cu grid (grid pitch =100 μm) covered with an elastic carbon membrane and dried at ambient temperature to prepare the specimen for TEM observation. Thermogravimetoric analysis (TGA) was performed by using TG-8310, RIGAKU, Japan. Synthesized Au NPs (5.67 mg) was placed on a Pt pan, and the sample was heated to 100 °C with its heating velocity of 10 °C/min. After keeping at 100 °C for 30 min to evaporate adsorbed water, the sample was heated up to 750 °C with its heating velocity of 10 °C/min. After acquisition of TGA curve, the

dx.doi.org/10.1021/ma200994q |*Macromolecules* 2011, 44, 5868–5873

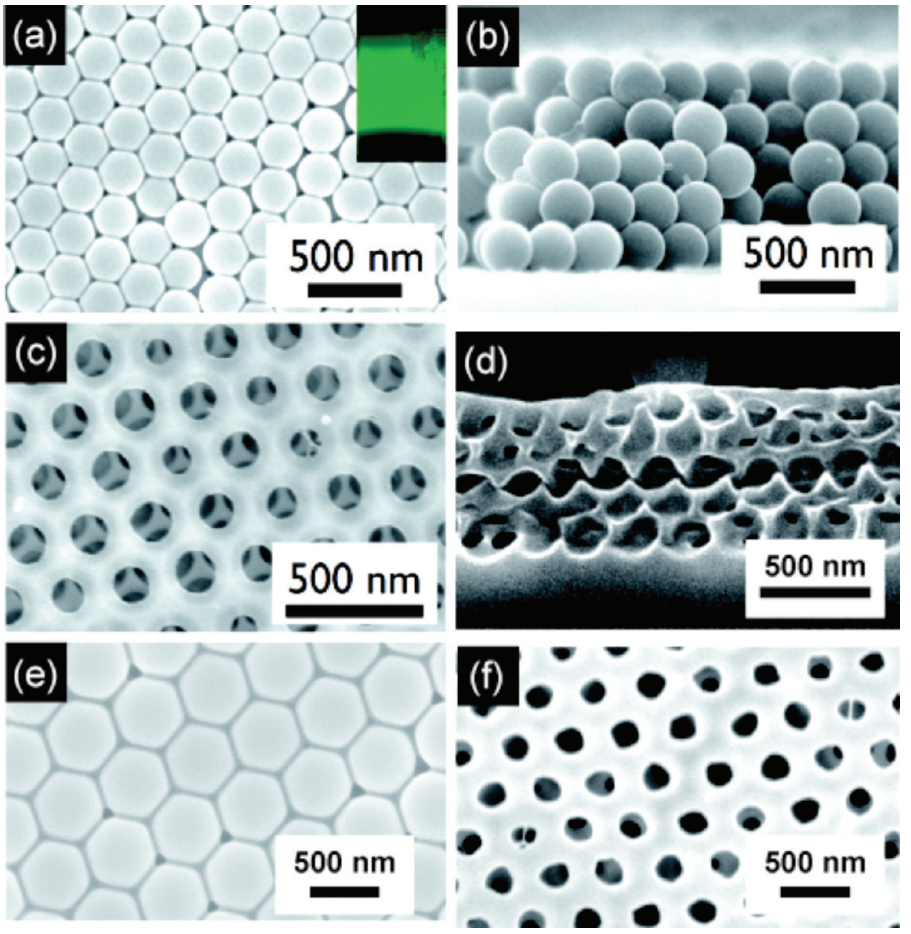

Figure 2. (a) FE-SEM images of a 248 nm PS colloidal crystal, (b) a cross section of PS colloidal crystal, (c) an inverse opal, (d) a cross section of an inverse opal, and (e) 498 nm PS colloidal crystals and an inversed opal of it, respectively.

sample was cooled to the room temperature. (See Supporting Information, part S4.)

2.2. Preparation of PS Colloidal Crystals and PVA Inverse Opals. Glass substrates (6.6 mm ×6.6 mm) were sonicated in acetone for 15 min, and then treated with UV−O_3 (OC-250615-D+A, Iwatani, Japan). The cleaned glass substrate was soaked in KOH aqueous (15 wt %) for 2 h, and then washed with Millipore membrane filtered (Milli-Q) water. The equipment for coating the colloidal crystals onto the glass substrate was composed of two moving substrate holders (Figure 1a(i));[28] the first glass plate was placed in a substrate holder, which moved smoothly at a speed set by a computer-controlled driving system. The second glass plate was held in the other substrate holder. The glass plates overlapped by about 4 cm and were separated by a gap of ∼200 μm. An aqueous dispersion of PS particles (0.1−0.4 wt %, diameter 244 ± 6 nm, or 498 ± 9 nm, Duke Scientific Corp) was added to the gap between the two glass substrates, and the bottom glass substrate was moved linearly at a speed of 1 μm/s. A thin liquid film of the colloidal dispersion and the meniscus were continuously formed in front of the edge of the upper glass substrate, and the PS colloidal particles were deposited on the bottom glass substrate after the water had evaporated (Figure 1a(ii)). The sample was then annealed at 75 °C for 30 min in a vacuum oven. The surface structures of the colloidal crystals were analyzed by field-emission scanning electron microscopy (FE-SEM, S-5200, Hitachi, Japan). The sample was cut into 2 mm × 3 mm specimens and Os was sputtered onto the surface (osmium coater, Shinku Device, Ibaraki, Japan). The Os-coated specimen was attached to an Al sample holder with carbon adhesive tape. The sample was observed at an acceleration voltage of 5 kV.

A low concentration aqueous solution of PVA (1 wt %, Wako Chemical Industries, Inc., Japan) was applied to the annealed colloidal crystals and dried at room temperature overnight. A high concentration aqueous solution of PVA (10 wt %) was applied to the colloidal crystals and dried to make the film rigid (Figure 1b(ii)). The specimen was immersed in chloroform for 2 days to remove the PS colloidal particles. The PVA inverse opal film was removed from the substrate, and washed with chloroform (Figure 1b(iii)). The surface structure of the film was also analyzed by FE-SEM using the same sample preparation procedure described above.

2.3. Introduction of Block Copolymers and Au Nanoparticles into PVA Inverse Opals. Poly(styrene-*block*-1,4-isoprene) (PS-*b*-PI, $M_{n(PS)}$ = 16.5 kg/mol, $M_{n(PI)}$ = 30.5 kg/mol, M_w/M_n = 1.08, f_{PI} = 0.74, Polymer Source Inc., Canada). PS-*b*-PI and the Au nanoparticles were dissolved in chloroform to prepare a 20 mg/mL solution (PS-*b*-PI:Au nanoparticles =3:7 weight ratio). The solution was applied to the PVA inverse opal film and dried at room temperature (Figure 1b(iv)). The solvent was allowed to evaporate, and the film was immersed in water at 50 °C to remove the template PVA film (Figure 1b(v)). The surface structure of the film was analyzed by FE-SEM using the same

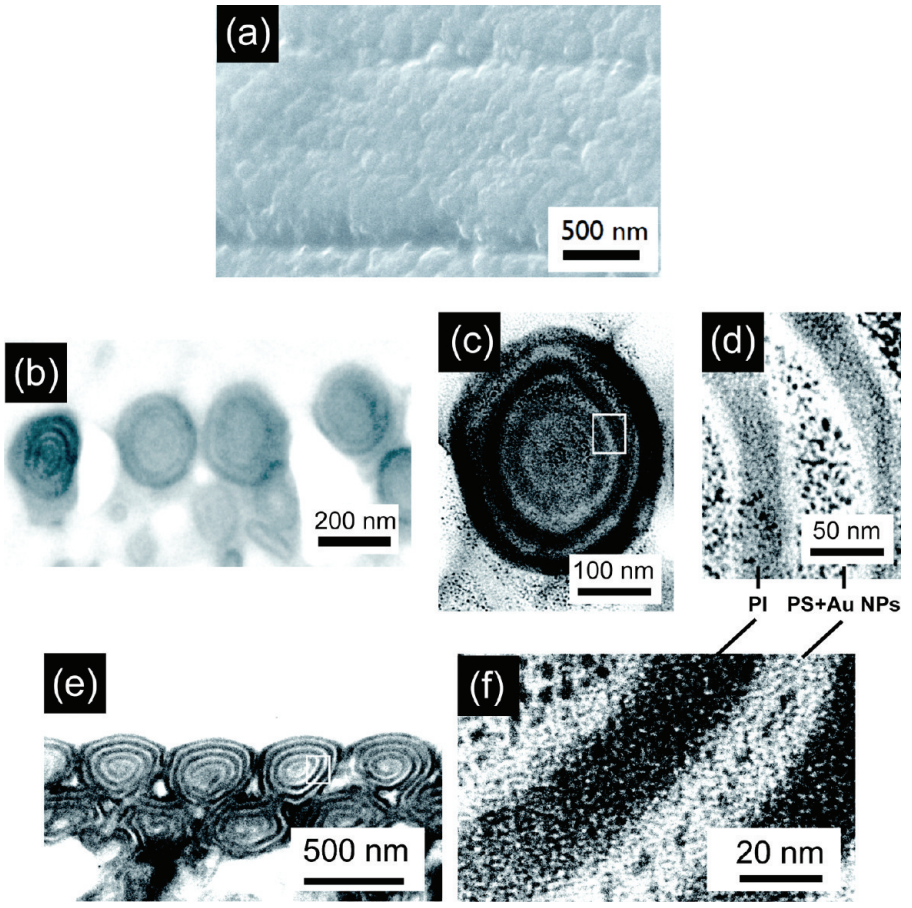

Figure 3. (a) FE-SEM image of Au nanoparticles and block copolymer composite filled in an inversed opal prepared from 248 nm PS colloidal crystals, (b) cross-sectional, and close-up cross-sectional TEM images of (c) Au nanoparticles, (d) block copolymer composite, and (e, f) cross-sectional images of Au nanoparticles and block copolymer composites filled in an inversed opal prepared from 498 nm PS colloidal crystals, respectively.

sample preparation procedure described above. The inner microphase separation structure of the film was observed by TEM. The PI moieties in the film were stained with OsO_4 vapor. The samples were embedded in epoxy resin (Epok-812, Wako Pure Chemical Industries, Ltd., Japan), and ultrathin specimens (100 nm) were prepared using an ultramicrotome (EM UC-6, Leica, Germany).

3. RESULTS AND DISCUSSION

Au nanoparticles were successfully synthesized, and a deep red chloroform dispersion was obtained. The absorption peak from the surface plasmon resonance was observed at 501 nm. The average diameter of the Au core was 3.6 nm, as measured in a TEM image (see Supporting Information, Figures S1 and S2). There are several methods for estimate the length of polymer chans adhered on nanoparticles. From the literature,[29] the Froly length and the coil-like model give the shortest and longest chain lengths, respectively. The estimated chain length differences between these two models increased with increasing molecular weights of polymers. In this experiment, since the M_n of the PS was low (M_n = 3.0 kg/mol), there is no significant change in the estimated polymer length by using these two models. The total diameter, which includes the length of the polymer chain, which stabilizes the PS moieties, was theoretically calculated as 9 nm by using the Flory length of the polymer chain.

A typical FE-SEM image of a colloidal crystal, prepared from 248 nm PS colloidal particles is shown in Figure 2a. A uniform fcc colloidal crystal was formed; the characteristic bright green color caused by the Bragg reflection was observed (Figure 2a (inset)). The heat treatment at 75 °C made the particles stick to each other[30] because the glass transition temperature of the PS colloidal particle's surface is lower than that of the bulk state.[31] A cross-sectional FE-SEM image of the colloidal crystal reveals that a multilayered structure was formed (Figure 2b). The number of colloidal layers was between 2 and 5, and was controlled by changing the concentration of solution from 0.1 wt % up to 0.4 wt % (see Supporting Information, Figure S3). A PVA inverse opal was prepared by using the colloidal crystals as templates. Figure 2c shows a top-down FE-SEM image of the hexagonally arranged submicrometer pores in the PVA inverse opal. The cross-sectional image of the inverse opal shows an interconnected multilayered porous structure (Figure 2d). The same colloidal crystals (Figure 2e) and PVA inversed opals (Figure 2f) were successfully prepared from 498 nm PS colloidal particles.

Figure 3a shows an FE-SEM image of an Au nanoparticles/PS-*b*-PI composite array; the spherical submicrometer structure reflecting the structure of the inverse opal template prepared from 248 nm PS colloidal particles. The cross-sectional image of the Au nanoparticles/PS-*b*-PI composite array also shows that spherical domains were formed in the film (Figure 3b). The close-up image of the single spherical domain shows onion-like

dx.doi.org/10.1021/ma200994q |*Macromolecules* 2011, 44, 5868–5873

microphase separation structures, consisting of gray PI phases and bright PS phases (Figure 3c). When the inner structure was more closed, black dots were observed in the PS phases, which were identified as Au nanoparticles (Figure 3d). The cross-sectional images of an Au nanoparticles/PS-*b*-PI composite array prepared from 498 nm PS particles are shown in Figure 3, parts e and f. In this case, the multilayered structures of spherical domains were clearly observed, and the periodicity of each microphase-separated structure is basically same as that in the 248 nm case. The array of Au nanoparticles are clearly imaged at PS phase (Figure 3f).

An onion-like microphase separation structure was formed, even though the f_{PI} value for PS-*b*-PI is 0.74. The thermodynamically stable microphase separation structure of this block copolymer is PS cylinders dispersed in a PI matrix.[32] We have found that morphologies of inner phase separation structures of block copolymer particles can be controlled by amount of blended metal nanoparticles.[33] From the TGA measurement, the synthesized Au nanoparticles containing free PS-SH molecules. Because the PS-SH-stabilized Au nanoparticles and free PS-SH molecules were incorporated into the PS phase, the volume fraction of the PS phase increased, and a lamellar microphase separation structure was formed. The microphase separation structures of block copolymers in 3D confinement spaces are affected by the size of the confinement spaces and the affinity of the polymer segments for the template materials. Experimental analysis of 3D confinement systems in block copolymer particles[34] and Monte Carlo simulations[35] indicate that when the ratio between the periodicity of a microphase separation structure (L_0) and the diameter of the confinement space (D) (D/L_0) is smaller than 2.0, frustrated phases appear. These phases are different from the microphase separation structures observed in the bulk system. When the affinity (α) of one of the polymer segments in the block copolymer used for the confinement space material, is higher than that of the other segments, the microphase separation structure is arranged along the interface between the domain of the block copolymer and the confinement space. In this case, the D value (249 nm) was sufficiently larger than L_0 to prevent the frustrated phase from appearing.

It is noteworthy that Au nanoparticles locatd along to the interface between the PVA matrix and the block copolymer phase (Figure 3c). There are two considerable reasons for this localization; one is segregation from the block copolymer phase, the other is ampihpihlic property of Au nanoparticles. During the solvent evaporation, the block copolymers constructed microphase separation structures including Au nanoparticles and free PS-SH, however, the excess Au nanoparticles were segregated from the microphase separation, as the result, the Au nanoparticles were located at the interface between the PVA matrix and the block copolymer phase. Moreover, it is well-known that nanoparticles have amphipihlic properties.[34] The ampihpihlic Au nanoparticles may also stabilize the interface.

4. CONCLUSION

In this paper, we reported a novel method for the 3D arrangement of metal nanoparticles. PS colloidal crystals were fabricated on glass substrates using a simple coating process, and PVA inverse opals were prepared by molding PS colloidal crystals. By embedding PS-*b*-PI and PS-stabilized Au nanoparticles into the pores of the PVA inverse opals, Au nanoparticles were three dimensionally arranged in onion-like microphase separation structures, formed in the spherical domains of the PVA inverse opals.

It has been reported that a unique microphase separation structure can be prepared in 3D confinement systems. Our method could be used to introduce various kinds of inorganic nanoparticles, such as noble metals, semiconductors, and metal oxides into three dimensionally arranged microphase separation structures. These organic−inorganic composite materials could be used in plasmonic devices, metamaterials, or lasers.

■ ASSOCIATED CONTENT

Ⓢ Supporting Information. TEM image of Au nanoparticles (Figure S-1), UV−vis absoption spectrum of Au nanoparticles (Figure S-2), cross-sectional SEM images of colloidal crystals (Figure S-3), and TGA curves of synthesized Au nanoparticles. This material is available free of charge via the Internet at http://pubs.acs.org.

■ AUTHOR INFORMATION

Corresponding Author

*Telephone and Fax: +81-22-217-5329. E-mail: yabu@tagen.tohoku.ac.jp.

■ ACKNOWLEDGMENT

H.Y. would like to thank Prof. H. Jinnai, Kyushyu University, and Dr. T. Arita, IMRAM, Tohoku University, for productive discussion regarding TEM and TGA measurement, respectively. This research is partially supported by Grant-in-Aid for Scientific Research on Innovative Areas "Metamaterials" (No. 23109502) of the Ministry of Education, Culture, Sports, Science and Technology, Japan.

■ REFERENCES

(1) Kim, K.; Lee, H. B.; Choi, J.-Y.; Shin, K. S. *ACS Appl. Mater. Inter.* **2011**, *3* (2), 324.

(2) Hentschel, M.; Saliba, M.; Vogelgesang, R.; Giessen, H.; Paul Alivisatos, A.; Liu, N. *Nano Lett.* **2010**, *10* (7), 2721.

(3) (a) Yeo, J.; Tsai, K.-T.; Wang, Y.; Liu, Z.; Bartal, G.; Wang, Y.-L.; Zhang, X. *Opt. Express* **2009**, *17* (25), 22380. (b) Helgert, C.; Rockstuhl, C.; Etrich, C.; Menzel, C.; Kley, E.-B.; Tuennermann, A.; Lederer, F.; Pertsch, T. *Phys. Rev. B* **2009**, *79*, 233107.

(4) Luk'yanchuk, B.; Zheludev, N. I.; Maier, S. A.; Halas, N. J.; Nordlander, P.; Gieesen, H.; Chong, C. T. *Nat. Mater.* **2010**, *9* (9), 707.

(5) Zhu, Z.; Meng, H.; Liu, W.; Liu, X.; Gong, J.; Qiu, X.; Jiang, L.; Wang, D.; Tang, Z. *Angew. Chem., Int. Ed.* **2011**, *50* (7), 1593.

(6) Bao, K.; Mirin, N. A.; Nordlander, P. *Appl. Phys. A: Mater. Sci. Process.* **2010**, *100* (2), 333.

(7) Liu, N.; Guo, H.; Fu, L.; Kaiser, S.; Schweizer, H.; Giessen, H. *Nat. Mater.* **2008**, *7* (1), 31.

(8) Day, J. K.; Neumann, O.; Grady, N. K.; Harras, N. J. *ACS Nano* **2010**, *4* (12), 7566.

(9) Lee, S.-W.; Lee, K.-S.; Ahn, J.; Lee, J.-J.; Kim, M.-G.; Shin, Y.-B. *ACS Nano* **2011**, *5* (2), 897.

(10) Qiu, T.; Jiang, J.; Zhang, W.; Lang, X.; Yu, X.; Chu, P. K. *ACS Appl. Mater. Inter.* **2010**, *2* (8), 2465.

(11) (a) Goulet, P. J. G.; Aroca, R. F. *Anal. Chem.* **2007**, *79*, 2728. (b) Yang, Y.-G.; Liu, H.-G.; Chen, L.-J.; Chen, K.-C.; Ding, H.-P.; Hao, J. *Langmuir* **2010**, *26* (18), 14879.

(12) Lohmueller, T.; Bock, E.; Spatz, J. P. *Adv. Mater.* **2008**, *20*, 2297.

(13) Stannard, A. *J. Phys.: Condens. Matter* **2011**, *23*, 083001.

(14) Isozaki, K.; Ochiai, T.; Taguchi, T.; Nittoh, K.-I.; Miki, K. *Appl, Phys. Lett.* **2010**, *97*, 221101.
(15) Cheng, W.; Camplongo, M. J.; Cha, J. J.; Tan, S. J.; Umbach, C. C.; Muller, D. A.; Lio, D. *Nat. Mater.* **2009**, *8* (6), 519.
(16) (a) Pavan, M. J.; Shenher, R. *J. Mater. Chem.* **2011**, *21* (7), 2028. (b) Lin, T.; Li, C. L.; Ho, R. M.; Ho, J. C. *Macromolecules* **2010**, *43* (7), 3383.
(17) Chang, J. Y.; Ross, C. A.; Thomas, E. L.; Smith, H. I.; Vancso, G. J. *Adv. Mater.* **2003**, *15* (19), 1599.
(18) Wu, Y. Y.; Cheng, G. S.; Katsov, K.; Sides, S. W.; Wang, J. F.; Tang, J.; Frederickson, G. H.; Moskovits, M.; Stucky, G. D. *Nat. Mater.* **2004**, *3* (11), 816.
(19) Koneripalli, N.; Singh, N.; Levicky, R.; Bates, F. S.; Gallagher, P. D.; Satija, S. K. *Macromolecules* **1995**, *28* (8), 2897.
(20) Xiang, H. Q.; Shin, K.; Kim, T.; Moon, S. I.; McCarthy, T. J.; Russell, T. P. *Macromolecules* **2004**, *37* (15), 5660.
(21) Arsenault, A. C.; Rider, D. A.; Téreault, N.; Chen, J. I. −L.; Coomns, N.; Ozin, G. A.; Manners, I. *J. Am. Chem. Soc.* **2005**, *127* (28), 9954.
(22) Dufresne, E. R.; Stark, D. J.; Greenblatt, N. A.; Cheng, J. X.; Hutchinson, J. W.; Mahadevan, L.; Weitz, D. A. *Langmuir* **2006**, *22* (17), 7144.
(23) Jiang, P.; McFarland, M. J. *J. Am. Chem. Soc.* **2004**, *126*, 13778.
(24) Kanai, T.; Sawada, T.; Toyotama, A.; Kitamura, K. *Adv. Funct. Mater.* **2005**, *15* (1), 25.
(25) Zhang, S.; Zhou, S.; You, B.; Wu, L. *Macromolecules* **2009**, *42* (10), 3591.
(26) Rider, D. A.; Chen, J. I. L.; Eloi, J.-C.; Arsenault, A. C.; Russell, T. P.; Ozin, G. A.; Manners, I. *Macromolecules* **2008**, *41* (6), 2250.
(27) Brust, M.; Fink, J.; Bethell, D.; Schiffrin, D. J.; Kiely, C. *J. Chem. Soc., Chem. Commun.* **1995**, 1655.
(28) Yabu, H.; Shimomura, M. *Adv. Func. Mater.* **2005**, *15* (4), 575.
(29) Leliévre, H. Y.; Desbiens, J.; Ritcey, A. M. *Langmuir* **2007**, *23*, 2843.
(30) Matsushita, S. I.; Shimomura, M. *Chem. Commun.* **2004**, 506.
(31) (a) Tanaka, K.; Takahara, A.; Kajiyama, T. *Macromolecules* **2000**, *33*, 7588. (b) Zhang, C.; Guo, Y.; Priestley, R. D. *Macromolecules* **2011**in press.
(32) Khandpur, A. K. *Macromolecules* **1995**, *28*, 8796.
(33) Yabu, H.; Koike, K.; Higuchi, T.; Shimomura, M. *Langmuir* **2011**submitted for publication.
(34) Higuchi, T.; Tajima, A.; Motoyoshi, K.; Yabu, H.; Shimomura, M. *Angew. Chem., Int. Ed.* **2008**, *47*, 8044.
(35) Yu, B.; Sun, P. C.; Chen, T. H.; Jin, Q. H.; Ding, D. T.; Li, B. H.; Shi, A. C. *J. Chem. Phys.* **2007**, *127*, 114906.